EuroSun2026

FROM NATURAL GAS TO HYDROGEN: AN INTEGRATED ENERGY HUB ANALYSIS FOR AN AUSTRIAN COFFEE ROASTERY

Nayrana Daborer-Prado, Aditi Dhakal, Gayaneh Issayan, Christian Wagner, Bernhard Zettl

University of Applied Sciences Upper Austria, Energy Research Group ASIC, Wels, Austria

Nayrana.Daborer-Prado@fh-wels.at

Summary

This paper presents the technical, operational, and economic results of a decarbonization approach for small industrial sites by integrating hydrogen (H_2). Applied to an Austrian coffee roastery use case, the simulation demonstrates how on-site green H_2 and renewables production can support a transition from natural gas. First, the performance of the integrated MATLAB/Simulink model is evaluated in terms of photovoltaic (PV) generation, H_2 production, storage energy demand and roasting heat supply. Subsequently, the optimization results are analyzed to assess electrolyzer operation, storage utilization, and grid-electricity consumption. Particular attention is given to the differences between low-pressure and high-pressure storage configurations. The resulting H_2-production and storage profiles are examined to identify key operational characteristics and constraints. A techno-economic evaluation is then performed using the Levelized Cost of Hydrogen (LCOH) as the primary performance indicator. Finally, sensitivity analyses are conducted to evaluate the influence of key technical and economic parameters on overall system feasibility.

Decarbonization, hydrogen H_2*, modeling and simulation, techno-economic evaluation*

Field of application for the findings: Energy planning and system modeling, industrial decarbonization, hydrogen H_2 *transition, multi-energy system integration.*

Addressed audience: Researchers and academics, industrial stakeholders, technology providers, network operators

1. Introduction

The decarbonization of industrial energy use has emerged as one of the principal challenges in achieving global climate mitigation targets. While substantial reductions in greenhouse gas emissions have been achieved in the electricity sector through the increasing deployment of renewable energy technologies, industrial process heat remains heavily dependent on fossil fuels, particularly natural gas (Leicher et al., 2024). This dependence is especially pronounced in small and medium-sized enterprises (SMEs), where limited financial resources, existing infrastructure lock-in, and strict operational reliability requirements often hinder the adoption of low-carbon technologies. In contrast, large industrial enterprises and energy-intensive sectors such as steel, chemicals, and refining have already developed decarbonization roadmaps and H_2-integration strategies (Leicher et al., 2024). Owing to their large H_2 demand, these industries are frequently prioritized in infrastructure planning, H_2-network development, and renewable-H_2 supply initiatives. Consequently, SMEs face additional challenges in accessing H_2 infrastructure and investment support, further emphasizing the need for decentralized and economically viable H_2 solutions tailored to smaller industrial users. In Europe, policy initiatives such as the European Green Deal, the Fit-for-55 package, and the EU H_2 Strategy have established ambitious pathways toward climate neutrality by 2050 and have identified renewable H_2 as a key technology for decarbonizing hard-to-abate industrial sectors (Vagnini et al., 2024; European Commission, 2019, 2020, 2021).

H_2 produced via water electrolysis using renewable electricity has received considerable attention as a versatile energy carrier capable of supporting sector coupling, renewable-energy integration, and industrial decarbonization. Compared with direct electrification, H_2 offers the advantage of long-term energy storage and can be gradually integrated (blending) into existing combustion-based industrial processes with relatively limited modifications. The rapid deployment of PV systems, declining electrolyzer costs, and supportive regulatory frameworks have accelerated interest in decentralized PV-H_2 systems for industrial applications. Nevertheless, the intermittent nature of solar energy introduces operational challenges associated with balancing renewable generation, H_2-production, compression, storage and end-use demand. As a result, the technical and economic performance of such systems depends strongly on their design, sizing, and operational strategy.

Integrated H_2-systems involve several interconnected subsystems operating across different physical domains, including electrical generation, electrochemical conversion, gas compression, storage, and thermal utilization. The interactions among these components cannot be adequately captured through individual component analyses alone. Instead, system-level modeling frameworks are required to quantify energy flows, evaluate operational flexibility, identify bottlenecks, and support investment decisions. Geidl and Andersson demonstrated the value of integrated multi-energy system modelling and emphasized the importance of optimization approaches for determining economically and technically optimal system configurations (Geidl et al., 2007; Geidl and Andersson, 2007b).

Recent research has increasingly combined physics-based simulation models with mathematical optimization techniques to improve the planning and operation of renewable-energy systems (Ożadowicz, 2025; Zhang et al., 2022). Physics-based models provide a detailed representation of thermodynamic, electrochemical and energy conversion processes, whereas optimization algorithms are used to identify operating strategies that minimize costs, maximize renewable-energy utilization, or reduce emissions. Among the available approaches, Linear Programming (LP) and Mixed-Integer Linear Programming (MILP) have become particularly attractive because of their computational efficiency and ability to represent operational constraints, storage dynamics and scheduling decisions. Simultaneously, dynamic simulation environments such as MATLAB/Simulink have become widely used for representing component-level behavior and transient system dynamics in renewable-powered H_2 applications (The MathWorks, Inc., 2026).

Although a substantial body of literature exists on H_2-production and techno-economic assessment, most studies have focused on large-scale industrial sectors (Silva et al., 2024; Povacz and Bhandari, 2023; Wolf et al., 2025). Furthermore, many studies evaluate individual technologies in isolation or employ simplified operational assumptions that do not fully represent the dynamic interactions between renewable electricity generation, H_2 production, storage behavior and industrial demand. Consequently, a significant research gap remains regarding integrated modeling and optimization frameworks for SME-scale industrial applications, where operational flexibility and economic constraints differ considerably from those of large industrial facilities.

Industrial coffee roasting provides a suitable case study for investigating these challenges. Coffee roasting is among the most energy-intensive processes within the coffee production chain and requires carefully controlled thermal energy at temperatures typically ranging between 180°C and 250°C (Pantaleo et al., 2018; Fabbri et al., 2011). Natural gas remains the dominant fuel due to its high energy density, controllability, and established industrial infrastructure. Previous studies reported carbon footprints ranging from approximately 0.74 to 0.80 $kg_{CO_2,eq}$ per kilogram of roasted coffee depending on the roasting technology and energy source (Tsai et al., 2025). Recent advances in H_2-compatible roasting technologies and burner systems have created opportunities to replace natural gas with renewable H_2 without requiring complete replacement of roasting equipment. However, the feasibility of such a transition depends on understanding the interactions among PV generation, electrolyzer operation, H_2 storage, and process heat demand throughout the year. To address these challenges, this study develops an integrated modeling and optimization framework for evaluating the replacement of natural gas with on-site renewable H_2 in an Austrian coffee roasting facility. The component-level models of PV generation, proton exchange membrane (PEM) electrolyzer, H_2 compression, storage and coffee roaster are implemented in MATLAB/Simulink and Simscape. Building on the latter simulation, an optimization is applied to determine optimal operational strategies and storage capacities while satisfying H_2 demand and minimizing annual operating costs. Particular attention is given to the interactions between renewable electricity utilization, grid-electricity consumption, storage operation, and H_2 production economics.

The primary contribution of this work is the integration of dynamic simulation and optimization within a unified decision-support framework for SME-scale industrial decarbonization. Unlike previous studies that focus solely on component performance or static techno-economic assessments, the proposed methodology simultaneously captures component-level dynamics, annual operational behaviour, storage management and economic performance. The developed framework provides insights into optimal system sizing, storage requirements, renewable-energy utilization, grid dependency, and the conditions under which on-site green

H_2 can become a technically feasible and economically competitive alternative to natural gas for industrial process-heat applications.

2. Modeling Methodology

The evaluation of the technical and economic feasibility of replacing natural gas with renewable H_2 in an coffee roasting facility is completed in multiple stages. The modeling and optimization framework consists of three interconnected MATLAB/Simulink models (The MathWorks, Inc., 2026) : (1) a PV-electrolysis system for on-site renewable H_2 production, (2) a multi-stage H_2 compression system for storage preparation, and (3) a lumped-parameter thermal model of a H_2-fired fluidized-bed coffee roaster. The simulation results flow subsequently in an optimization framework. The overall methodology is illustrated in Figure 1. The

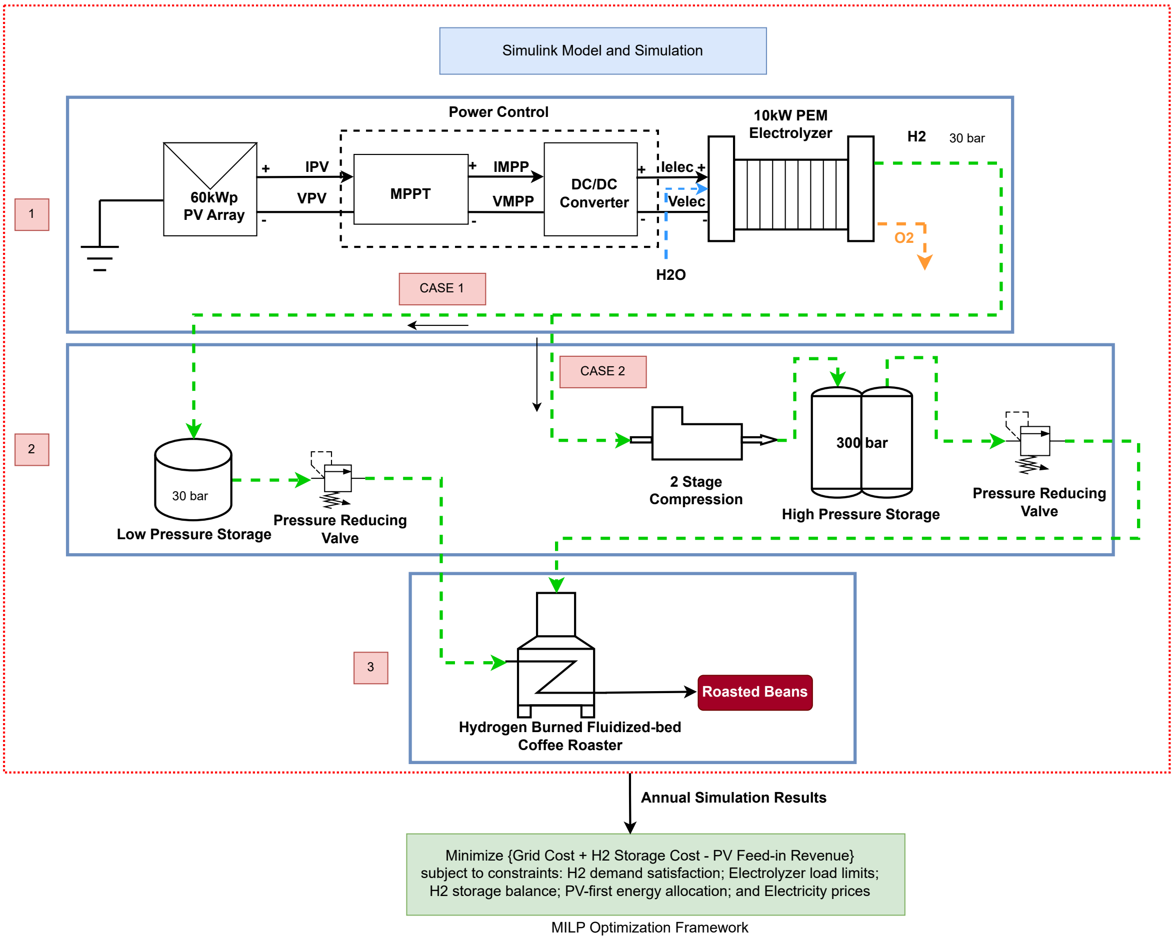

Fig. 1: Schematic overview of the integrated simulation and optimization framework, comprising of (1) PV-electrolysis, (2) multi-stage H_2 compression, and (3) H_2 coffee roaster model. The simulation outputs are used in a MILP-based optimization for optimal system operation and H_2-storage sizing.

simulation is driven by annual Solar irradiance data with an hourly temporal resolution is generated from PVGIS-ERA5 database for the selected site location (European Commission, Joint Research Centre, 2026). The PV system generates electrical power which is supplied to a PEM electrolyzer. The generated H_2 is subsequently compressed and stored according to the selected storage configuration. The resulting hourly electricity generation and H_2 production profiles are used as inputs to a MILP optimization framework. The optimization determines the optimal operating strategy and storage sizing while minimizing grid-electricity consumption and annualized storage costs subject to H_2-demand satisfaction and system-operating constraints. Finally, a techno-economic assessment is performed through the calculation of the Levelized Cost of Hydrogen (LCOH) for two storage configurations: low-pressure storage (Case 1) and high-pressure storage (Case 2).

2.1 PV-Electrolysis Model

The PV array was implemented using the Simscape Solar Cell block, which represents the solar cell using a photocurrent source combined with exponential diode components and parasitic resistive elements (MathWorks, 2026a).The PV array consists of 190 Trina Solar 320 W modules configured as 19 modules in series and 10 parallel strings, providing a total installed capacity of 60.8 kWp (Trina Solar, 2017). The generated electrical power is determined from the array voltage and current as described in Equation 1.

$$P_{\mathrm{PV}} = V_{\mathrm{PV}} I_{\mathrm{PV}} \tag{1}$$

P_{PV} is the PV power output, V_{PV} is the array voltage, and I_{PV} is the array current. Due to the nonlinear characteristics of PV arrays, a unique operating point exists at which the generated power reaches its maximum value, referred to as the Maximum Power Point (MPP) (Siddique et al., 2025). Since irradiance and temperature continuously vary throughout the year, MPP also changes dynamically. Therefore, a Maximum Power Point Tracking (MPPT) controller is required to ensure operation near the maximum-power condition. The PV system employs the Perturb and Observe (P&O) MPPT algorithm in conjunction with a DC-DC buck converter (Siddique et al., 2025). The measured PV voltage and current signals are processed by a MATLAB Function block implementing the P&O algorithm. A fixed perturbation step size of 0.0005 was adopted. The minimum and maximum allowable duty cycles were constrained to 0.2 and 0.45, respectively. Furthermore, an additional voltage-protection condition was incorporated into the controller to decrease the duty cycle whenever the electrolyzer voltage exceeded 160 V. To reduce computational effort and avoid modelling high-frequency switching behaviour, an average-value DC-DC buck converter model was implemented with an assumed conversion efficiency of 95%.

The output of the DC-DC converter is connected directly to the PEM electrolyzer stack. The electrolyzer is configured with 71 cells connected in series and operated at a stack voltage of approximately 158–160 V. The stack current is limited to 63.3 A, resulting in a nominal electrolyzer power rating of approximately 10 kW. For a PEM electrolyzer, water is supplied to the anode, where it is oxidized to oxygen gas, releasing protons H^+ and electrons (oxygen evolution reaction (OER)). Further, generated protons migrate through the polymer electrolyte membrane to the cathode, where they combine with electrons from the external circuit in H_2 evolution reaction (HER) to form H_2. Both oxidation OER and reduction HER reactions are presented in Equation 2 (Shiva Kumar and Himabindu, 2019).

$$\mathrm{H_2O} \rightarrow \frac{1}{2}\mathrm{O_2} + 2\mathrm{H^+} + 2e^- \qquad \Longrightarrow \qquad 2\mathrm{H^+} + 2e^- \rightarrow \mathrm{H_2} \tag{2}$$

The Simscape Electrolyzer block represents the stack as a lumped electrical load composed of multiple series-connected electrolysis cells. The electrical power consumed by the electrolyzer is calculated in Equation 3.

$$P_{\mathrm{el}} = V_{\mathrm{stack}} I_{\mathrm{stack}} \tag{3}$$

P_{el} is the electrical power input, V_{stack} is the stack voltage, and I_{stack} is the stack current. Water electrolysis occurs only when the supplied electrical energy exceeds the thermodynamic minimum energy requirement for water splitting. H_2 production is determined internally by the electrochemical model based on stack current and Faraday's law (Schalenbach et al., 2018).

2.2 Multi-Stage H_2 Compression Model

Storing the produced H_2 from the electrolyzer is implemented by compression to achieve sufficient volumetric energy density. As H_2 compression is an irreversible process associated with significant temperature rise, multistage compression with intercooling is required (Franco and Giovannini, 2024). In industrial applications, discharge temperatures are typically maintained below approximately 200°C to protect compressor components and ensure safe operation. Furthermore, compression ratios exceeding 7 per stage are generally undesirable, making multistage compression necessary for pressure levels above approximately 200 bar (Franco and Giovannini, 2024). In the present work, H_2 is compressed from an electrolyzer outlet pressure of 30 bar to a storage pressure of 300 bar. Consequently, a two-stage compression configuration is adopted. The energy required is estimated using the polytropic compression relation in following Equation 4 (Franco and Giovannini, 2024).

$$W_{\mathrm{comp}} = \frac{n}{n-1} R T_1 \left[\left(\frac{P_2}{P_1} \right)^{\frac{n-1}{n}} - 1 \right] \tag{4}$$

Here, W_{comp} is the specific compression work, R is the gas constant, T_1 is the inlet temperature, P_1 and P_2 are inlet and outlet pressures, respectively, and n is the polytropic exponent. The compressor electricity demand is incorporated into the overall system energy balance and subsequently included within the optimization framework.

2.3 H_2-Fired Coffee Roaster Model

The thermal demand of the roasting process is represented using a lumped-parameter model of a H_2-fired fluidized-bed coffee roaster developed based on the works of (Al-Shemmeri et al., 2025). The model is intended to capture the overall thermal dynamics and H_2 consumption profile rather than detailed fluid-flow behavior or combustion chemistry. Thermal energy is provided through H_2 combustion. The useful thermal power delivered to the roasting air is expressed in Equation 5.

$$\dot{Q}_{\text{useful}} = \eta_b \dot{m}_{\text{H}_2} \text{LHV}_{\text{H}_2} \tag{5}$$

$\dot{Q}_{\text{useful}}$ is the useful heat-transfer rate, η_b is the burner efficiency, $\dot{m}_{\text{H}_2}$ is the H_2 mass flow rate, and LHV_{H_2} is the lower heating value of H_2. The lower heating value of H_2 is assumed to be 120 MJ kg^{-1} and is used because water generated during H_2 combustion leaves the burner as vapor and its latent heat is not recovered.

The cumulative H_2 consumption over the roasting cycle is obtained using Equation 6.

$$m_{\text{H}_2,\text{tot}} = \int_0^t \dot{m}_{\text{H}_2} \, dt \tag{6}$$

A combined feedforward-feedback control strategy is employed to regulate H_2 consumption and maintain the desired roasting-air temperature profile. The feedforward component consists of a predefined H_2-flow lookup table representing the nominal roasting trajectory, while a second lookup table defines the desired temperature profile during the roasting cycle. The feedback controller adjusts the H_2-flow command to compensate for deviations between the actual and desired roasting-air temperatures.

2.4 MILP-Based Optimization Framework

The outputs of the dynamic MATLAB/Simulink models, including hourly PV generation, electrolyzer H_2 production, compressor electricity consumption, and roaster H_2 demand, are exported to a MILP optimization framework (MathWorks, 2026b). The optimization is performed over an annual horizon with hourly time resolution. The objective function shown in Equation 7 minimizes the annual cost of grid-electricity consumption C_{grid} and H_2-storage capacity C_{storage} while accounting for the revenue R_{export} generated from exporting surplus PV electricity:

$$\min Z = C_{\text{grid}} + C_{\text{storage}} - R_{\text{export}} \tag{7}$$

By minimizing Equation 7, the optimization determines the most cost-effective electrolyzer operating schedule and storage capacity while maximizing utilization of available PV generation and satisfying the H_2 demand of the coffee roasting process and respecting all system-operating constraints.

2.5 Economic Assessment

A final techno-economic assessment is performed using the optimized annual operating results. Low-pressure and high-pressure storage configurations are evaluated. The economic performance of each configuration is assessed using the LCOH (Agora Industry and Umlaut, 2023):

$$\text{LCOH} = \frac{\sum_{t=1}^{N} \frac{CAPEX_t + OPEX_t}{(1+r)^t}}{\sum_{t=1}^{N} \frac{m_{\text{H}_2,t}}{(1+r)^t}} \tag{8}$$

In Equation 8 the $CAPEX_t$ and $OPEX_t$ denote capital and operating expenditures, respectively, $m_{\text{H}_2,t}$ is the annual H_2 production, r is the discount rate, and N is the project lifetime. The resulting LCOH values are used to compare the economic feasibility of the low-pressure and high-pressure storage configurations and to assess the competitiveness of renewable H_2 as a replacement for natural gas in industrial coffee roasting.//

Techno-economic assessments of water electrolysis systems employ the LCOH methodology proposed by Agora Energiewende (Agora Industry and Umlaut, 2023), which annualized investment and operating costs over the useful lifetime of the system described below in Equation 9 with capital recovery factor (CRF) utilized.

$$\mathrm{LCOH} = \frac{\sum_i (CRF_i \cdot CAPEX_i) + OPEX_{\mathrm{fixed}} + C_{\mathrm{grid}} + C_{\mathrm{stack}} - R_{\mathrm{export}}}{m_{\mathrm{H_2,annual}}} \quad \text{with} \quad CRF = \frac{r(1+r)^n}{(1+r)^n - 1} \tag{9}$$

Here, with r denoting the discount rate or weighted average cost of capital (WACC), and n representing the component lifetime in years. In Equation 9, $CAPEX_i$ represents the capital expenditure of component i, $\sum_i(CRF_i \cdot CAPEX_i)$ is the total annualized capital cost of all system components, $OPEX_{\mathrm{fixed}}$ denotes the annual fixed operation and maintenance costs, C_{grid} is the annual cost of grid electricity consumption, C_{stack} is the annual stack replacement reserve, R_{export} represents the revenue obtained from exporting surplus PV electricity to the grid, and $m_{\mathrm{H_2,annual}}$ is the annual H_2 production. The LCOH is expressed in €/kg H_2 and provides a unified metric for comparing the economic performance of different H_2-production configurations.

3. Results and Discussion

The developed modelling and optimization framework was applied to evaluate the technical and economic feasibility of supplying a H_2-fired coffee roaster using on-site PV electricity and H_2 storage. The results are discussed in terms of system operation, H_2 production and storage behaviour, optimization outcomes, and the resulting H_2 production costs for the investigated storage configurations.

3.1 Optimization of Electrolyzer Operation and Storage Utilisation

Case 1: Low-Pressure H_2 **Storage** The optimized operation of the low-pressure (LP) storage configuration results in an annual H_2 production of 738 kg H_2, with monthly production remaining relatively uniform throughout the year. The optimization schedules electrolyzer operation according to a PV-first strategy, where available PV electricity is utilized whenever possible. Additional grid electricity is used only when required to satisfy H_2 demand and when electricity prices are sufficiently low. Figure 2 illustrates the optimized operating profile presented in black solid line. During daylight hours, H_2 production is primarily supplied by PV generation, while grid-assisted operation is shifted to periods with lower electricity prices. High-price periods are largely avoided unless required by H_2-demand, storage-capacity, or electrolyzer-operating constraints. This operating strategy minimizes grid-electricity costs while ensuring a reliable H_2 supply for the coffee roasting process.

Fig. 2: Average Daily Electrolyzer Operation showing PV-driven and Grid-driven operating hours for Case 1.

Case 2: High-Pressure H_2 **Storage** Here, the compressor adds the electrical load demand and consequently modifies the optimal hourly electricity allocation and H_2 production schedule. The resulting dispatch reflects the combined electricity requirements of electrolysis and compression together with high-pressure (HP) storage flexibility. Figure 3 shows that gid-supported production is shifted towards lower-price periods, including late-evening operation. Compared with Case 1, the additional compressor demand and lower HP-storage capacity penalty alter the economically preferred production hours.

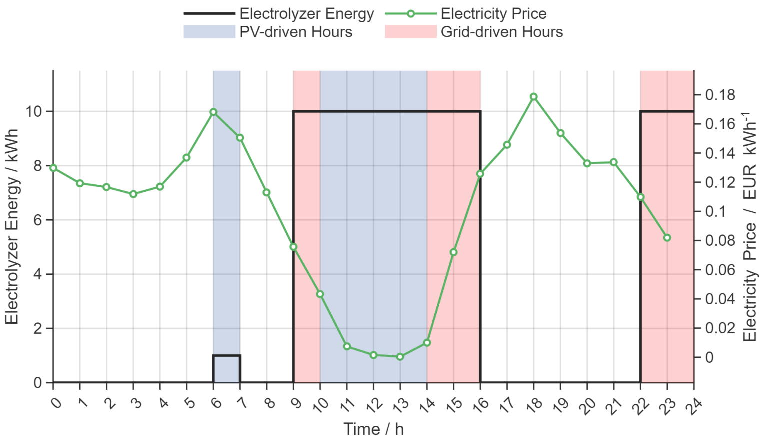

Fig. 3: Average daily electrolyzer operation showing PV-driven and grid-driven operating hours for Case 2.

Figure 4a and 4b show a clear seasonal shift in the electricity supply structure for both the cases. PV electricity supplied to the electrolyzer increases from approximately 500 kWh/month in winter to 1500-1700 kWh/month between May and September. This reduces the corresponding grid requirement during the high-irradiance period. The site loads follow the same PV-first allocation, with grid electricity supplying the residual demand after available PV has been utilized. Compressor electricity consumption is comparatively small throughout the year in Case 2, although being an additional consumer.

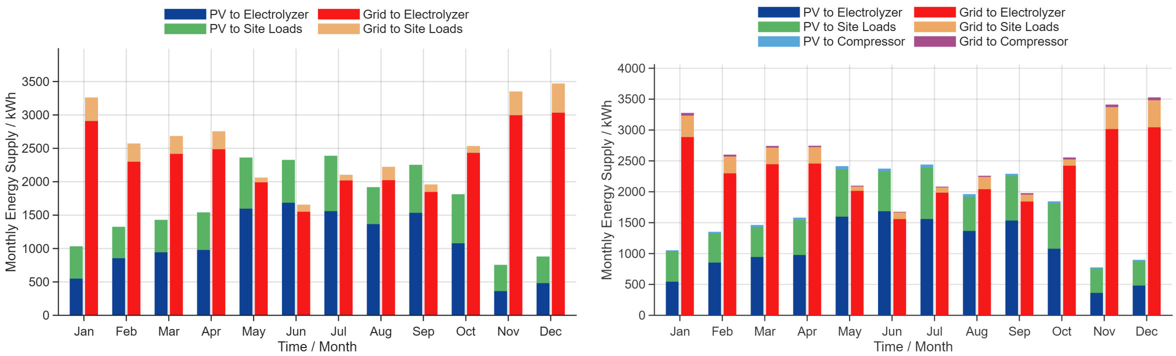

(a) Case 1: Low-pressure storage.

(b) Case 2: High-pressure storage.

Fig. 4: (a) Monthly PV and grid energy allocation to electrolyzer and site loads for Case 1 (b) added compressor operation loads for Case 2.

Figure 5 presents the storage behavior of both the LP and HP storage configurations under the optimized operating schedules. In both cases, H_2 is accumulated during non-roasting periods and withdrawn during roasting operations to satisfy process demand. The HP configuration achieves a higher storage inventory and requires a peak storage capacity of 7.6 kg H_2, compared to 6.9 kg H_2 for the LP configuration. This difference is a direct result of the optimization objective and storage-cost formulation. Owing to its lower annualized storage-capacity cost, the HP system can economically store larger quantities of H_2 and concentrate production during the most favorable operating periods. In contrast, the LP configuration tends to produce H_2 closer to the time of consumption, resulting in less storage utilization and a greater dependence on electricity-price conditions during operating hours. Overall, the optimization demonstrates that storage-cost assumptions significantly influence the temporal distribution of H_2 production and storage utilization, while both configurations successfully satisfy the annual H_2 demand of the coffee roastery.

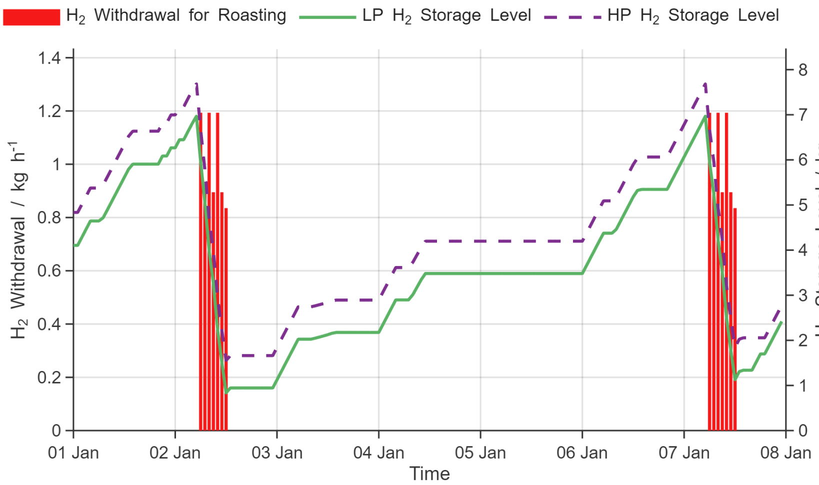

Fig. 5: Storage behavior of both Case 1: LP and Case 2: HP storage configurations under the optimized operating schedules in a representative week.

3.2 Economic and sensitivity analysis

A one-at-a-time (OAT) sensitivity analysis was conducted to assess the influence of key techno-economic parameters on the LCOH. Each parameter was varied by ±20% while all other parameters were kept at their baseline values. The resulting effects on the LCOH for Cases 1 and 2 are presented in Figure 6 and Figure 7. For both storage configurations, the discount rate, PV CAPEX, and electrolyzer CAPEX were identified as the most influential parameters. In Case 1, which has a base LCOH of 21.11 €/kg H_2, the discount rate produced the largest variation, followed by PV and electrolyzer investment costs. Parameters related to equipment lifetime exhibited a moderate impact, whereas electrolyzer specific energy consumption (SEC), storage cost, and storage lifetime had only a minor influence on the H_2 cost. A similar sensitivity ranking was observed for Case 2, with a base LCOH of 20.80 €/kg H_2. Overall, the tornado analysis indicates that the economics of both H_2-storage configurations are primarily driven by capital investment and financing assumptions, while technical-performance and storage-related parameters contribute comparatively less to the overall LCOH uncertainty.

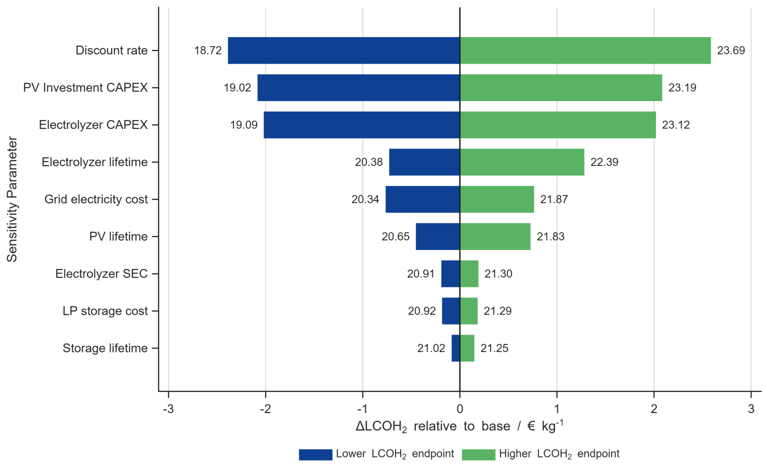

Fig. 6: Sensitivity analysis of LCOH for Case 1: LP with ±20% parameter variations. PV CAPEX, electrolyzer CAPEX, and the discount rate are identified as the primary cost drivers.

A two-parameter sensitivity analysis was performed to investigate the combined influence of electrolyzer CAPEX and H_2-storage cost on the LCOH. Both parameters were varied simultaneously between 50% and 150% of their baseline values, and the resulting LCOH values for Cases 1 and 2 are presented in Figure 6 and Figure 7. For both storage configurations, electrolyzer CAPEX was found to have a substantially greater impact on LCOH than storage cost. In Case 1, the LCOH varied between 15.60 and 26.61 €/kg H_2 across the investigated parameter range, while Case 2 exhibited a similar range of 15.40 to 26.19 €/kg H_2. Changes

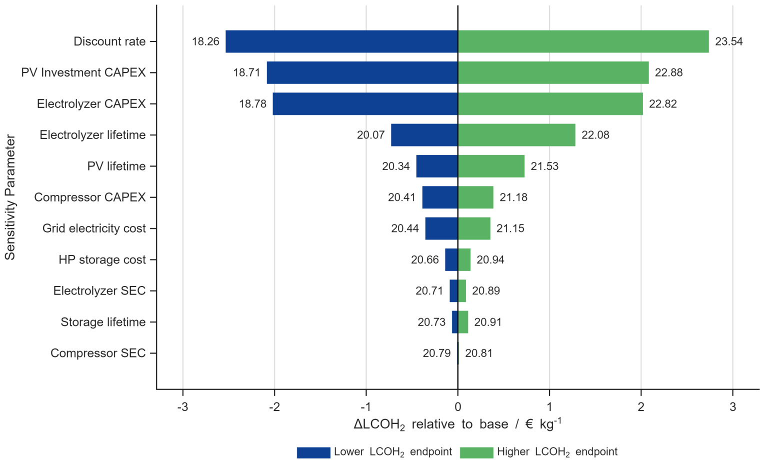

Fig. 7: Sensitivity analysis of LCOH for the Case 2: HP with ±20% parameter variations. PV CAPEX, electrolyzer CAPEX, and the discount rate are more pronounced as the primary cost drivers compared to Case 1.

in electrolyzer investment cost resulted in pronounced variations in H_2 production cost, whereas variations in storage cost had a comparatively minor effect.

Overall, the results confirm that the economic performance of both storage scenarios is driven primarily by electrolyzer investment costs. The contribution of storage cost remains relatively small, even when combined with significant variations in electrolyzer CAPEX, indicating that cost reductions in electrolyzer technology are likely to have a much greater impact on future H_2 competitiveness than reductions in storage-system costs.

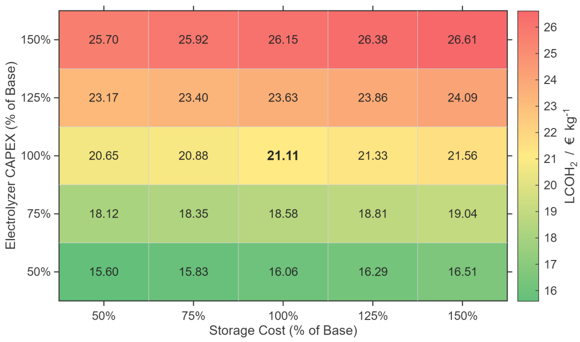

(a) Case 1: LP storage.

(b) Case 2: HP storage.

Fig. 8: Heatmap of LCOH for (a) Case 1: LP and (b) Case 2 HP storage as a function of electrolyzer CAPEX and H_2-storage cost Both parameters are varied ±50% of their baseline values.

4. Conclusion

This study developed an integrated modeling and optimization framework for evaluating the replacement of natural gas with renewable H_2 in an Austrian coffee roasting facility. Detailed MATLAB/Simulink models of PV generation, PEM electrolysis, H_2 compression, storage, and H_2-fired roasting were coupled with an MILP-based optimization framework to determine optimal system operation and storage sizing. The optimization successfully identified operating strategies that prioritized the utilization of locally generated PV electricity while satisfying the H_2 demand of the roasting process. The results confirmed the system is technically feasible: the optimized hybrid PV-grid design meets 100% of the roastery's annual H_2 demand, with rooftop PV supplying approximately 37% of that demand directly and grid-supported electrolysis reliably closing the remainder. Peak on-site storage requirements were modest, at 6.9-7.6 kg depending on configuration.

The economic analysis revealed that the LCOH is dominated by capital-related expenditures, with electrolyzer CAPEX emerging as the single most influential parameter. This reflects the economic challenges associated with small-scale H_2 production systems, where limited H_2 throughput results in relatively high specific investment costs. In contrast, H_2-storage costs and other technical parameters had a considerably smaller impact on the overall H_2 production cost. Despite the relatively high calculated LCOH values, the proposed system offers advantages when compared with the purchase of externally supplied green H_2. On-site H_2 production reduces dependency on external supply chains, avoids transportation and distribution costs, and enables direct utilization of locally available renewable electricity. As electrolyzer costs continue to decline and renewable electricity generation becomes increasingly affordable, the economic competitiveness of decentralized H_2 production for SME applications is expected to improve.

The analysis suggests that the proposed system can become both technically and economically competitive with externally purchased H_2 under future cost-reduction scenarios. The heatmaps demonstrates that a 25% reduction in electrolyzer CAPEX already yields a noticeable improvement in economic feasibility, while a 50% reduction leads to substantially lower H_2 production costs and significantly improved long-term competitiveness. These findings highlight the importance of continued cost reductions in electrolyzer technology and indicate that subsidy mechanisms could play a critical role in enabling SMEs to transition towards renewable H_2-based process heat solutions.

Overall, the results demonstrate that renewable H_2 can technically replace natural gas in industrial coffee roasting and that optimization-based operation is essential for maximizing renewable-energy utilization and minimizing operating costs. Future work should investigate larger system scales, alternative electricity-market conditions, dynamic electricity pricing, and emerging electrolyzer technologies to further improve the economic viability of on-site green H_2 production.

References

Agora Industry and Umlaut. Levelised cost of hydrogen: Making the application of the lcoh concept more consistent and more useful. Technical Report 301/01-S-2023/EN, Agora Energiewende, Berlin, Germany, 2023. URL https://www.agora-energiewende.org/fileadmin/Projekte/2022/2022-12-10_Trans4Real/A-EW_301_LCOH_WEB.pdf. Accessed: 2026-07-01.

K. W. Ahmed, M. J. Jang, M. G. Park, Z. Chen, and M. Fowler. Effect of components and operating conditions on the performance of pem electrolyzers: A review. *Electrochem*, 3(4):581–612, Sept. 2022. ISSN 2673-3293. doi: 10.3390/electrochem3040040.

M. Al-Shemmeri, P. J. Fryer, R. Farr, and E. Lopez-Quiroga. Batch-scale simulation of heat and mass transfer of coffee roasting in spouted bed roasters. *Beverages*, 11(6):162, Nov. 2025. ISSN 2306-5710. doi: 10.3390/beverages11060162.

J. D. Bustos-Vanegas, M. A. Martins, P. C. Corrêa, F. M. Baptestini, and G. H. H. d. Oliveira. Modeling and simulation of coffee bean heating during roasting: Effect of heat generation. *Frontiers in Food Science and Technology*, 5, May 2025. ISSN 2674-1121. doi: 10.3389/frfst.2025.1603783.

European Commission. The european green deal, 2019. URL https://eur-lex.europa.eu/legal-content/EN/TXT/?uri=CELEX:52019DC0640.

European Commission. A hydrogen strategy for a climate-neutral europe, 2020. URL https://eur-lex.europa.eu/legal-content/EN/TXT/?uri=CELEX:52020DC0301.

European Commission. 'fit for 55': Delivering the eu's 2030 climate target on the way to climate neutrality, 2021. URL https://eur-lex.europa.eu/legal-content/EN/TXT/?uri=CELEX:52021DC0550.

European Commission, Joint Research Centre. Photovoltaic geographical information system (pvgis), 2026. URL https://re.jrc.ec.europa.eu/pvg_tools/en/. Accessed: 2026-04-01.

A. Fabbri, C. Cevoli, L. Alessandrini, and S. Romani. Numerical modeling of heat and mass transfer during coffee roasting process. *Journal of Food Engineering*, 105(2):264–269, 2011. doi: 10.1016/j.jfoodeng.2011.02.030.

A. Franco and C. Giovannini. Hydrogen gas compression for efficient storage: Balancing energy and increasing density. *Hydrogen*, 5(2):293–311, May 2024. ISSN 2673-4141. doi: 10.3390/hydrogen5020017.

M. d. l. A. Franco and K. Bartl. Carbon footprint of the coffee roasting process based on two technologies with different sources of energy in peru. *European Journal of Sustainable Development*, 7(3), July 2018. ISSN 2239-6101. doi: 10.14207/ejsd.2018.v7n3p90.

M. Geidl and G. Andersson. Optimal coupling of energy infrastructures. In *2007 IEEE Lausanne Power Tech*, pages 1398–1403. IEEE, July 2007a. doi: 10.1109/PCT.2007.4538520.

M. Geidl and G. Andersson. Optimal power flow of multiple energy carriers. *IEEE Transactions on Power Systems*, 22(1):145–155, Feb. 2007b. ISSN 1558-0679. doi: 10.1109/TPWRS.2006.888988.

M. Geidl, G. Koeppel, P. Favre-Perrod, B. Klöckl, G. Andersson, and K. Fröhlich. Energy hubs for the future. *IEEE Power and Energy Magazine*, 5(1):24–30, Jan. 2007. ISSN 1540-7977. doi: 10.1109/MPAE.2007.264850.

P. Koštial, I. Špička, Z. Jančíková, J. David, J. Valíček, M. Harničárová, and V. Rusnák. Lumped capacitance model in thermal analysis of solid materials. *Journal of Physics: Conference Series*, 588:012006, Feb. 2015. ISSN 1742-6596. doi: 10.1088/1742-6596/588/1/012006.

J. Leicher, A. Giese, and C. Wieland. Electrification or hydrogen? the challenge of decarbonizing industrial (high-temperature) process heat. *J*, 7(4):439–456, Oct. 2024. doi: 10.3390/j7040026.

MathWorks. Solar cell. Simscape Electrical Documentation, 2026a. URL `https://www.mathworks.com/help/sps/powersys/ref/solarcell.html`. Accessed: 2026-04-03.

MathWorks. intlinprog: Mixed-integer linear programming (milp). MATLAB Optimization Toolbox Documentation, 2026b. URL `https://www.mathworks.com/help/optim/ug/intlinprog.html`. Accessed: 2026-06-28.

A. Ożadowicz. Modeling and simulation tools for smart local energy systems: A review with a focus on emerging closed ecological systems' application. *Applied Sciences*, 15(16):9219, Aug. 2025. ISSN 2076-3417. doi: 10.3390/app15169219.

A. M. Pantaleo, R. Fordham, et al. Integrating cogeneration and intermittent waste-heat recovery in food processing: Microturbines vs. orc systems in the coffee roasting industry. *Applied Energy*, 225:782–796, 2018. doi: 10.1016/j.apenergy.2018.04.097.

L. Povacz and R. Bhandari. Analysis of the levelized cost of renewable hydrogen in austria. *Sustainability*, 15(5):4575, Mar. 2023. ISSN 2071-1050. doi: 10.3390/su15054575.

H. Sayed-Ahmed, A.-I. Toldy, and A. Santasalo-Aarnio. Dynamic operation of proton exchange membrane electrolyzers—critical review. *Renewable and Sustainable Energy Reviews*, 189:113883, Jan. 2024. ISSN 1364-0321. doi: 10.1016/j.rser.2023.113883.

M. Schalenbach, A. R. Zeradjanin, O. Kasian, S. Cherevko, and K. J. J. Mayrhofer. A perspective on low-temperature water electrolysis – challenges in alkaline and acidic technology. *International Journal of Electrochemical Science*, 13(2):1173–1226, Feb. 2018. ISSN 1452-3981. doi: 10.20964/2018.02.26.

S. Shiva Kumar and V. Himabindu. Hydrogen production by pem water electrolysis – a review. *Materials Science for Energy Technologies*, 2(3):442–454, Dec. 2019. ISSN 2589-2991. doi: 10.1016/j.mset.2019.03.002.

M. A. B. Siddique, D. Zhao, and A. U. Rehman. Emerging maximum power point control algorithms for pv system: Review, challenges and future trends. *Electrical Engineering*, 107(8):9807–9839, Feb. 2025. ISSN 1432-0487. doi: 10.1007/s00202-025-03002-0.

H. G. Silva, A. A. Merrouni, S. Touili, and J. Neto. Determination of photovoltaic hydrogen production potential in portugal: A techno-economic analysis. *Frontiers in Energy Research*, 12, July 2024. ISSN 2296-598X. doi: 10.3389/fenrg.2024.1380543.

The MathWorks, Inc. Matlab, 2026. URL `https://www.mathworks.com`.

Trina Solar. Tsm-pd14: 320–335 wp polycrystalline module – datasheet, 2017. Technical datasheet.

W.-H. Tsai, K.-H. Lee, and C.-C. Huang. Energy efficiency and carbon emission reduction in coffee roasting: Approach of activity-based costing (abc) methodology. *Energies*, 18(5):1018, Feb. 2025. ISSN 1996-1073. doi: 10.3390/en18051018.

C. Vagnini, L. C. Vieira, M. Longo, and M. Mura. Regional drivers of industrial decarbonisation: A spatial econometric analysis of 238 eu regions between 2008 and 2020. *Regional Studies*, 59(1), Aug. 2024. ISSN 1360-0591. doi: 10.1080/00343404.2024.2380369.

N. Wolf, R. Neuber, A. Mädlow, and M. Höck. Techno-economic analysis of green hydrogen supply for a hydrogen refueling station in germany. *International Journal of Hydrogen Energy*, 106:318–333, Mar. 2025. ISSN 0360-3199. doi: 10.1016/j.ijhydene.2025.01.424.

Y. Zhang, B. Vand, and S. Baldi. A review of mathematical models of building physics and energy technologies for environmentally friendly integrated energy management systems. *Buildings*, 12(2):238, Feb. 2022. ISSN 2075-5309. doi: 10.3390/buildings12020238.

Acknowledgment

The authors acknowledge the financial support provided through the project BioH2Region – Competence Region for Renewable Hydrogen and Green Gases (Project No. BA0100157), funded under the Interreg VI-A Bavaria–Austria 2021–2027 Program and co-financed by the European Union.

Appendix: Parameters

Tab. 1: Techno-economic parameters used in the analysis.

Parameter	Base Value	Unit
Discount Rate	6	%
PV Capacity	60	kWp
PV CAPEX	1,000	€/kWp
PV Lifetime	25	years
PV O&M	5	% CAPEX/yr
Electrolyzer CAPEX	60,000	€
Electrolyzer Lifetime	20	years
Electrolyzer O&M	2	% CAPEX/yr
Stack Replacement Share	25	% ELY CAPEX
Stack Durability	60,000	full-load hours
Electrolyzer SEC	55.52	kWh/kg H_2
Compressor CAPEX	10,000	€
Compressor Lifetime	15	years
Compressor O&M	4	% CAPEX/yr
Compressor SEC	1.05	kWh/kg H_2
Low-Pressure Storage Cost	1,000	€/kg H_2
High-Pressure Storage Cost	683.8	€/kg H_2
Storage Lifetime	20	years
Storage O&M	1	% CAPEX/yr
Feed-in Tariff	0.045	€/kWh